



Fly ash-based geopolymer as a potential adsorbent for Cr(VI) removal

Jingping Qiu, Yingliang Zhao*, Jun Xing, Xiaogang Sun

College of Resources and Civil Engineering, Northeastern University, Shenyang, 110819, China,
emails: zhao-yingliang@outlook.com (Y. Zhao), qiujingping@mail.neu.edu.cn (J. Qiu), xingjun@mail.neu.edu.cn (J. Xing),
sunxiaogang@mail.neu.edu.cn (X. Sun)

Received 16 July 2016; Accepted 7 January 2017

ABSTRACT

A novel adsorbent was prepared by fly ash (FA) via geopolymerization and used for the removal of Cr(VI) from aqueous solutions. The preparation condition was optimized through an orthogonal array test, using a NaOH/Na₂SiO₃ mass ratio of 2.0, an alkali activator/FA mass ratio of 0.5 and a curing temperature of 60°C. Then batch experiments were carried out to investigate the effects of various experimental parameters such as initial solution pH, adsorbent dosage, contact time, initial Cr(VI) concentration and interfering ions on the removal efficiency. The adsorption kinetics were fitted well by a pseudo-second-order model. The applicability of the Langmuir and Freundlich models for the adsorption data was tested. It was found that the adsorption isotherms followed Freundlich isotherm model better than the Langmuir isotherm in the temperature range between 298 and 318 K. The highest adsorption capacity occurred at 298 K, reaching a value of 49.751 mg/g. Furthermore, the adsorption process was found to be exothermic and more favorable at lower temperatures.

Keywords: Fly ash-based geopolymer; Cr(VI) adsorption; Kinetics; Isotherms

1. Introduction

Cr(VI) ion is considered to be one of the heavy metal pollutants in wastewater that are hazardous to human health and to the environment [1,2]. Removal of heavy metal ions can have short-term and long-term effects on human health [3,4]. Many effective methods have been reported to remove heavy metal ions from water systems, including chemical precipitation, ion exchange, electrochemical treatment and adsorption [5–7]. Adsorption in particular has advantages over other methods due to its low cost, high efficiency and regenerative ability [8–11].

The amount of fly ash (FA) released by factories and thermal power plants keeps increasing throughout the world. Therefore, the disposal of FA has become a serious environmental and economic issue [12–14]. In recent years, only about 20%–30% of the generated FA is used, mainly as an additive in cement and concrete and as filling material

in mining goaf filling, while the rest is discarded [15–17]. Therefore, strategies to deal with FA are required.

It is well known that FA has a porous structure, and the porosity can range from 60% to 70%. In addition, FA has the property of high specific surface area, so it has a relative strong adsorption ability [18,19]. However, since FA is powdered, it is difficult to be used in an adsorption column. Moreover, its dissatisfactory adsorptive property also restricts the industrial application of FA-based adsorbent. As a result, preparing FA into an adsorbent with high efficiency and low cost to deal with sewage water waste is a topic of recent interest. Synthesis of zeolite using FA as raw material to make an adsorbent is one route [4,20–22]. However, this process needs high temperature and high pressure, which increases the cost and restricts its large-scale application. Therefore, it is urgent to explore a new adsorbent preparation method of FA-based adsorbent.

Geopolymer is an inorganic material based on the polymerization of silicon and aluminium tetrahedral precursors in high alkaline media with the alkali or alkaline

* Corresponding author.

earth metal cations providing charge balance to the Al(IV) coordinated anion [23–26]. The structure of the geopolymer is porous and is similar to zeolite [27–31], which shows potential to be a new kind of adsorbent. To the authors' knowledge, there are few and very limited studies on the utilization of geopolymer to remove heavy metal ions. Medpelli et al. [7] explored the removal capabilities of arsenic using iron oxide-modified nanoporous geopolymer. Luukkonen et al. [6] used metakaolin as a raw material to synthesize the geopolymer, which was then applied to remove ammonium from model solutions and landfill leachate. Al-Harahsheh et al. [3] synthesized the geopolymer from waste FA as adsorbent for copper from aqueous solutions.

In this paper, an FA-based geopolymer adsorbent (FAGA) was prepared. The effects of NaOH/Na₂SiO₃ mass ratio, alkali activator dosage and curing temperature on the adsorption of Cr(VI) ions were studied. Also, the optimum preparation conditions were investigated by using the Taguchi method. Then, scanning electron microscopy (SEM), X-ray diffraction (XRD) analysis, Fourier transfer infrared (FTIR) spectrometer analysis and N₂ adsorption analysis were carried out to explore the properties of FAGA prepared under the optimal conditions. Batch adsorption experiments aimed to investigate the influencing factors of adsorption efficiency.

2. Materials and methods

2.1. Source materials

FA was collected from thermal power plants in Henan, China, and used as source materials to synthesize geopolymer-based adsorbent. The chemical composition of FA as measured by X-ray fluorescence (XRF) was: SiO₂ = 54.79%, Al₂O₃ = 23.57%, Fe₂O₃ = 1.13% and CaO = 1.07%. The average particle size and specific surface area were 29–32 μm and 0.76 m²/g, respectively. The alkali activator was a mixture of 12 mol/L NaOH solution and Na₂SiO₃ (SiO₂ = 26.5 wt%, Na₂O = 8.3 wt%, H₂O = 65.2 wt%). The Cr(VI) ion solution was prepared by dissolving K₂Cr₂O₇ (analytical grade standard) in distilled water and further diluted to concentrations required for the experiment.

2.2. Geopolymer preparation

Geopolymer was prepared by mixing FA and the alkali activator for 5 min in order to obtain a homogenous slurry before pouring into steel molds. The molds were vibrated for 2 min to remove entrained air bubbles. After that, the molds were sealed with polyethylene film and cured for 28 d. Thereafter, geopolymer were washed using distilled water to remove the excess alkali, and then crushed to 0.5–1 mm.

2.3. Characterizations

XRD analysis was carried out using X-ray diffractometer. The scanning range of 2θ was between 5° and 90°. A ZEISS scanning electron microscope was used at accelerating voltage of 10 kV. SEM measurements were performed on the geopolymer particles by evaporating gold on the surface. Surface area and pore size distribution were collected using a Brunauer, Emmert and Teller (BET) equation with N₂ as a

carrier gas. The concentration of Cr(VI) was determined by inductively coupled plasma optical emission spectrometry (ICP-OES).

2.4. Batch adsorption tests

Batch adsorption tests were carried out to explore the effects of FAGA dosage, pH, contact time, temperature, initial Cr(VI) concentration and interfering ions.

The percentage removal efficiency (*R*) was calculated using the following equation [32]:

$$R = \frac{C_0 - C_e}{C_0} \times 100\% \quad (1)$$

where *C*₀ and *C*_{*e*} are the initial and equilibrium concentration (mg/L) of Cr(VI), respectively.

The quantity of Cr(VI) uptake (*Q*_{*t*}, mg/g) by the FAGA was determined as [33]:

$$Q_t = \frac{C_0 - C_e \times V}{m} \quad (2)$$

where *V* and *m* are the solution volume (L) and FAGA dosage (g), respectively.

3. Result and discussion

3.1. Optimum of FAGA preparation

The alkali activator is an important parameter during the synthesis of geopolymer. Aluminosilicate materials are dissolved in alkali solution. On the other hand, alkali metal cations must be present in the cavities of the geopolymer network to balance the negative charge [34]. Therefore, the composition of the alkali activator greatly influences the properties of the geopolymer. Curing temperature is also an important parameter during the synthesis of geopolymer and is a reaction accelerator [35]. However, a higher curing temperature does not necessarily lead to a high performance product [36].

Based on the above analysis, NaOH/Na₂SiO₃ mass ratio, alkali activator dosage and curing temperature were explored using an L16 (4⁴) orthogonal array. The experiment details are shown in Table 1. The effect of combinations of these factors and levels was assessed by the removal efficiency of Cr(VI) at a temperature of 298 K using an FAGA dosage of 2.0 g/L for a contact time of 100 min. The initial concentration of Cr(VI) and pH value were 40 mg/L and 5, respectively. The results are presented in Table 2.

Table 1
Factors and levels for L16 (4⁴) orthogonal array

Factor	Level			
	1	2	3	4
NaOH/Na ₂ SiO ₃ (mass ratio)	1	2	3	4
Alkali activator/FA (mass ratio)	0.3	0.4	0.5	0.6
Curing temperature (°C)	20	40	60	80

Table 2
L16 (4⁴) orthogonal array for optimization of FAGA preparation

No.	A	B	C	Removal efficiency (%)
1	1	1	1	56.12
2	1	2	2	67.22
3	1	3	3	75.45
4	1	4	4	66.17
5	2	1	2	69.15
6	2	2	1	74.11
7	2	3	4	86.12
8	2	4	2	90.16
9	3	1	3	80.15
10	3	2	4	84.56
11	3	3	1	76.17
12	3	4	2	66.19
13	4	1	4	63.98
14	4	2	3	61.45
15	4	3	2	66.10
16	4	4	1	58.12
K_1	264.96	269.40	264.51	
K_2	319.54	287.34	268.66	
K_3	307.06	303.83	307.21	
K_4	249.65	280.64	300.83	
R	17.48	8.61	10.68	
Optimal plan	A2	B3	C3	

Analysis of the orthogonal array data suggests that A2B3C3 (NaOH/Na₂SiO₃ mass ratio of 2, alkali activator/FA mass ratio of 0.5 and curing temperature of 60°C) was the optimal combination of factors and levels. Therefore, FAGA prepared using the conditions of A2B3C3 was used for the Cr(VI) adsorption.

3.2. Characterization

The XRD patterns of FA and FAGA are shown in Fig. 1. The main crystalline phases in FA were quartz, mullite, albite and anorthite. But an amorphous structure could be observed from the background peak in the region of $2\theta = 15^\circ\text{--}30^\circ$. After geopolymerization, the intensity of the initial crystalline phases (quartz, mullite, albite and anorthite) decreased, and a new phase (N-A-S-H) was observed. A broad peak in the region $2\theta = 20^\circ\text{--}40^\circ$ was also observed from the XRD pattern of FAGA, which indicates the occurrence of geopolymerization occurred [37], in agreement with previous reported works [38–40].

Fig. 2 shows the FTIR spectra of FA and FAGA. The most characteristic difference observed between the FTIR spectrum of FA and FAGA is the band resulted from the

asymmetric stretching vibrations of T–O–Si (T = Al or Si). This band appeared at about 1,067 cm⁻¹ in the FTIR spectrum of FA but shifted to lower frequencies (997 cm⁻¹) in the FTIR spectra of FAGA indicating the formation of a new product (N-A-S-H) [41]. Al-Zboon et al. [42] found similar results where this band appeared at 1,035 cm⁻¹ and shifted to lower frequencies (<100 cm⁻¹). The disappearance of the absorption band at about 800 cm⁻¹ contributed to the AlO₄ vibrations and the appearance of new bands between 780 and 580 cm⁻¹ related to the symmetric stretching vibrations of T–O–Si (T = Al or Si), in the FAGA are further evidence of the formation of N-A-S-H [43–45].

The pore size distribution of FAGA (Fig. 3) is in the range of about 2–160 nm with an average pore diameter of 6.34 nm. The pore volume of FAGA was found to be 0.022 cm³/g. The BET surface area of FAGA was found to be 4.58 m²/g in comparison with the BET surface area of FA, which was 0.35 m²/g. This increase of the BET surface area in the FAGA vs. that of FA was due to the porous structure of FAGA. Therefore,

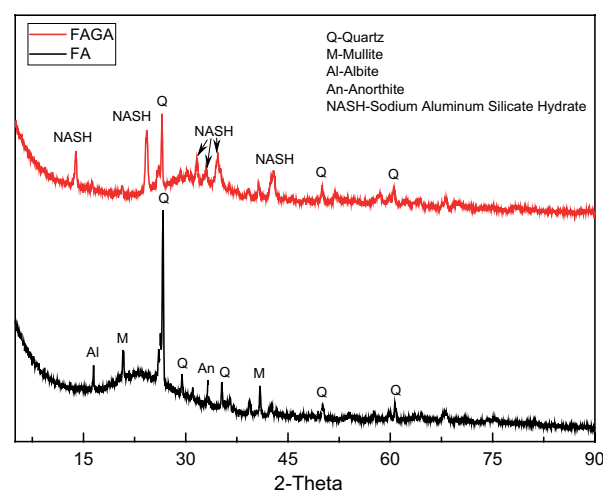


Fig. 1. XRD pattern of FA and FAGA.

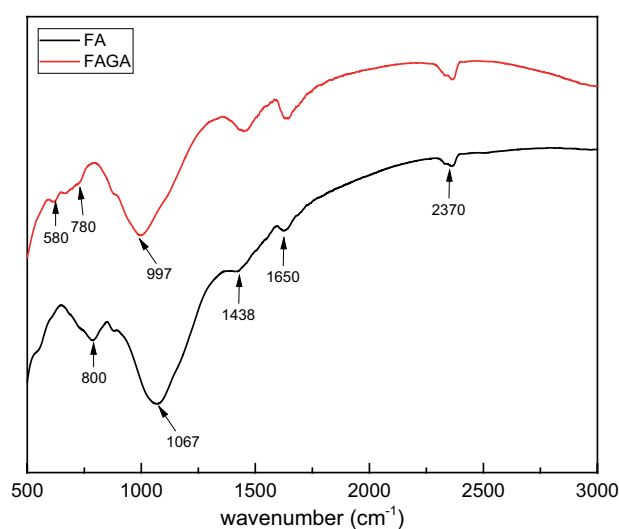


Fig. 2. FTIR spectra of FA and FAGA.

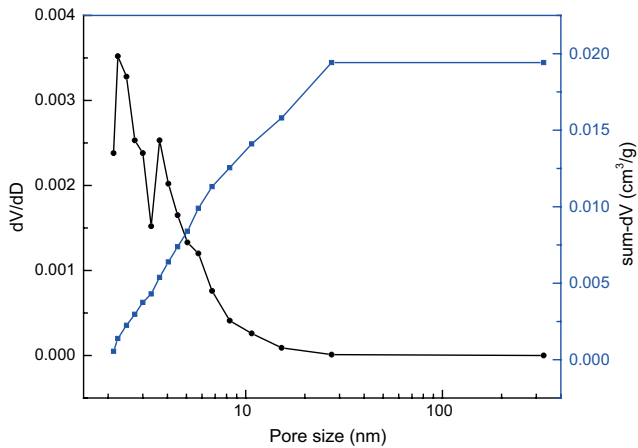


Fig. 3. Pore-size distribution of FAGA.

the porous structure of the FAGA would favor the adsorption of heavy metal ions [46].

3.3. Adsorption kinetics

The adsorption capacities of FAGA were measured as a function of contact time in order to explore the optimum contact time between the FAGA and Cr(VI). Therefore, 0.2 g of FAGA was added into 100 mL of Cr(VI) solution with a concentration of 40 mg/L at a pH = 5 and 298 K. The result is shown in Fig. 4(a). It is clear from Fig. 4(a) that the amount of Cr(VI) adsorbed increased as a function of contact time and reached equilibrium after 100 min, after which it remained constant. Fig. 4(a) shows that a significant removal of Cr(VI) occurred within the first 60 min (87.85%) and only a slight change occurred after 60 min. Liu [47] found that the equilibrium contact time for Cr(VI) absorption by ultrafine FA was around 80 min. Similar results were also obtained by Al-Zboon et al. [33], where the maximum removal of Pb(II) ions by FA-based geopolymer was achieved after 1 h.

The pseudo-first-order and pseudo-second-order kinetic models given by Eqs. (3) and (4) [3], respectively, were used to fit the experimental data in Fig. 4(a):

$$\text{First order: } \ln(Q_e - Q_t) = \ln Q_e - K_1 t \quad (3)$$

$$\text{Second order: } \frac{t}{Q_t} = \frac{1}{K_2 Q_e^2} + \frac{t}{Q_e} \quad (4)$$

where k_1 and k_2 are the first-order and second-order adsorption rate constants, respectively. Q_e and Q_t are the adsorption capacity (mg/g) at equilibrium and at time t . The fitting results are shown in Figs. 4(b) and (c), and the corresponding kinetic adsorption parameters are listed in Table 3.

It can be seen from Table 3 that the correlation coefficient for the pseudo-second-order kinetic model ($R^2 = 0.997$) is higher than for the pseudo-first-order kinetic model ($R^2 = 0.941$). In comparison with the pseudo-first-order, the theoretical Q_e value (19.417 mg/g) of the pseudo-second-order kinetic model is much close to the experimental data.

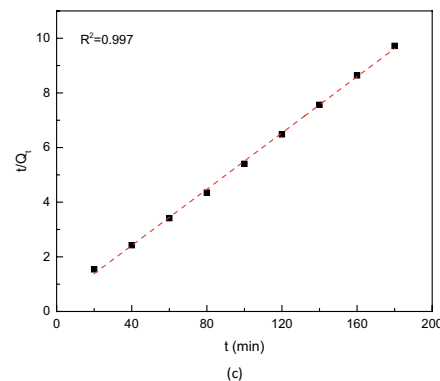
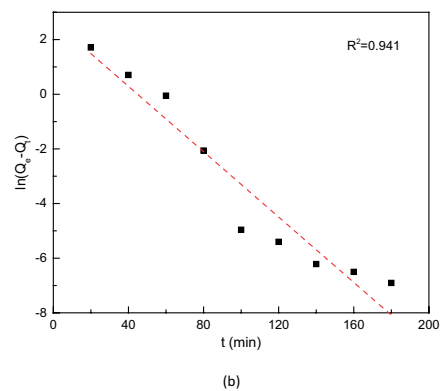
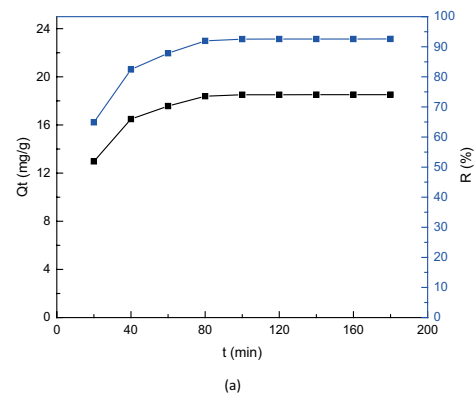


Fig. 4. (a) Adsorption kinetics of FAGA toward Cr(VI); (b) pseudo-first-order model; and (c) pseudo-second-order model.

Table 3
Kinetics parameters

Pseudo-first-order			Pseudo-second-order		
k_1	Q_e (mg/L)	R^2	k_2	Q_e (mg/L)	R^2
0.067	11.592	0.941	0.007	19.417	0.997

Therefore, the adsorption process between the FAGA and Cr(VI) fits a pseudo-second-order adsorption model. Similar results were also found by other researchers. For example, Ge et al. [48] found that the removal of Cu(II) ions from aqueous

solutions using porous geopolymeric spheres as adsorbent followed a pseudo-second-order kinetic model. Al-Zboon et al. [42] used a natural volcanic tuff-based geopolymer for Zn removal and reported that pseudo-second-order model showed the best fit of the experimental data.

3.4. Adsorption isotherms and thermodynamics

Adsorption isotherms are essential to investigate the nature of the interaction between Cr(VI) and FAGA. Two isotherm models were used in this study to quantify the adsorption capacity of FAGA at different temperatures and various Cr(VI) concentration. First, 0.2 g of FAGA was added

into 100 mL of Cr(VI) solution with a concentration of 20, 40, 60, 80, 100 and 120 mg/L at a pH of 5. Then vibrated for 100 min at three different temperatures (298, 308 and 318 K). The results are shown in Fig. 5.

The most common description of the adsorption capacity is through the empirical models of adsorption via the Freundlich and Langmuir equations. The Langmuir and Freundlich isotherm models are given by Eqs. (5) and (6) [33], respectively, and were used to evaluate the experimental data:

$$\text{Langmuir isotherm model: } \frac{1}{Q_e} = \frac{1}{Q_m} - \frac{1}{K_L Q_m} \frac{1}{C_e} \quad (5)$$

$$\text{Freundlich isotherm model: } \ln Q_e = \ln K_F + \frac{1}{n} \ln C_e \quad (6)$$

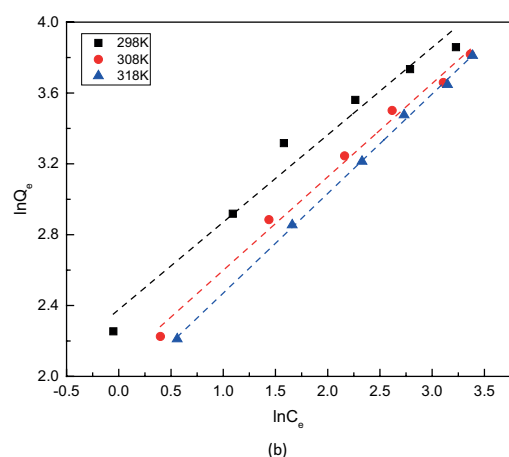
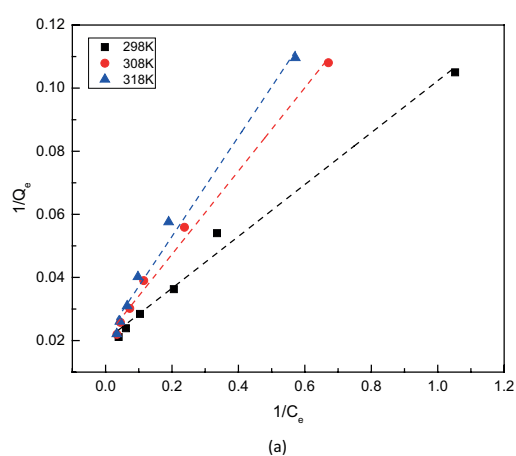


Fig. 5. (a) Langmuir isotherm model and (b) Freundlich isotherm model.

where Q_m is the monolayer capacity of the adsorbent; K_L is the Langmuir adsorption constant; K_F and n are the Freundlich constants.

The Langmuir model is mainly appropriate for homogeneous adsorption process, where the adsorption of each adsorbate molecule onto the surface has equal adsorption activation energy [49], and it assumes a monolayer coverage absorption. While the Freundlich model is applicable to describe heterogeneous systems, reversible adsorption is not restricted to the formation of monolayers [49].

Langmuir and Freundlich parameters for adsorption of Cr(VI) are listed in Table 4. As seen from Table 4, the value of K_L is between 0 and 1 indicating that the adsorption process is favorable. The correlation coefficient (R^2) values of Freundlich isotherm model are higher than those of Langmuir isotherm model, which suggests that the adsorption data are better described by the Freundlich isotherm model. This indicates that the adsorption of Cr(VI) on the surface of FAGA is heterogeneous and there is interaction between adsorbed molecules [33]. There are different active sites on the surface of FAGA, and the binding capacities with Cr(VI) of these sites are different. Previous research [50] has also reported similar result. On the other hand, the value of K_F decreased as the temperature increased indicating that the adsorption process is more favorable in lower temperature [8,51]. This is in agreement with the results of the Langmuir isotherm model, which showed that the maximum capacity (Q_m) decreased as the temperature increased. The maximum adsorption capacities of some adsorbents used for the removal of Cr(VI) as reported are shown in Table 5. It can be seen from Table 5 that the adsorption capacity of the FAGA is higher than most of those materials. The experimental conditions may not be the

Table 4
Isotherms parameters

Temperature (K)	Langmuir isotherm model			Freundlich isotherm model		
	Q_m (mg/g)	K_L (L/mg)	R^2	n	K_F (L/mg)	R^2
298	49.751	0.245	0.963	2.028	9.776	0.985
308	47.847	0.158	0.937	1.896	7.937	0.971
318	46.729	0.135	0.910	1.779	7.242	0.951

same as those of the current work, but the higher adsorption capacity of the FAGA suggests that it shows potential to be a promising adsorbent for wastewater treatment of Cr(VI).

The values of Gibbs free energy (ΔG°), enthalpy (ΔH°) and entropy (ΔS°) of the adsorption process were calculated using the following equations [33]:

$$\Delta G^\circ = \Delta H^\circ - T\Delta S^\circ \quad (7)$$

$$\ln K_F = -\frac{\Delta H^\circ}{RT} + \frac{\Delta S^\circ}{R} \quad (8)$$

where T and R are the temperature (K) and thermodynamic constant (8.314 J/K·mol), respectively. The results are presented in Fig. 6 and Table 6.

From Table 6, the negative values of ΔG° indicate that the adsorption of Cr(VI) was an feasible and spontaneous process [53]. Furthermore, ΔG° increases as a function of temperature, which suggests that the adsorption process is exothermic and that this process is more favorable at lower temperatures [54], in agreement with the adsorption isotherm analysis. Similar type of behavior has been reported earlier [3,55].

The exothermic behavior of the adsorption process is also supported by the fact that the values of ΔS° are negative suggesting that the system entropy decreases after the adsorption process. Adsorption of Cr(VI) on the surface of FAGA leads to the combination of Cr(VI) binding to the active sites of FAGA that results in a decrease of the system disorder and reduces its entropy.

The value of ΔH° is -13.936 kJ/mol, indicating that the adsorption of Cr(VI) by FAGA is a entropy-reducing process [56]. According to Open et al. [48], the adsorption types could be determined through the value of ΔH° , which are listed in Table 7. As seen from Table 7, the adsorption of Cr(VI) onto FAGA occurs mainly through hydrogen bond and dipolar bond force-based process, not a chemical bond-based process [18].

3.5. The effect of pH

The pH value is one of the most important factors for adsorption processes, which affects not only the surface charge of the adsorbents but also the form of Cr(VI). The effect of different initial pH values (2–9) of Cr(VI) solution on its removal efficiency was studied at a temperature of 298 K using an FAGA dosage of 2.0 g/L for a contact time of 100 min. The initial concentration of Cr(VI) was 40 mg/L, and the result is presented in Fig. 7.

Table 5
Comparison of adsorption capacity of FAGA with other adsorbents for Cr(VI) removal

Adsorbents	Q_m (mg/g)	Equilibrium time (min)	References
FAGA	49.751	100	Present work
PPy-HNTs clay NC	149.25	5–30	[52]
Spent activated clay	1.422	100	[51]
Chitosan-coated fly ash	33.27	50	[8]
HCl-AC	7.47	1,440	[11]

Note: PPy-HNTs NC – polypyrrole-coated halloysite nanotube nanocomposite; and HCl-AC – HCl activated Akadama clay.

As shown in Fig. 7, the removal efficiency of Cr(VI) is strongly influenced by the pH of the initial solution. The removal efficiency increases with the increase of pH up to 5 (82.01% at pH of 2 to 92.55% at pH of 5), after which it decreases with the increase of pH.

The main forms of Cr(VI) that exist are CrO_4^{2-} , $\text{Cr}_2\text{O}_7^{2-}$ and HCrO_4^- , which are determined by the pH of solution and the concentration of Cr(VI) [53,57,58]. In this study, the concentration of Cr(VI) was 40 mg/L with a pH range of 2–9, so the dominant forms of Cr(VI) that exist in the system were CrO_4^{2-} and HCrO_4^- . At acidic conditions, Cr(VI) exists in the solution in the form of HCrO_4^- . When the pH of the solution is lower than the isoelectric point of FAGA, protonation takes place at the surface of FAGA. This process could gather positive charge, which could attract HCrO_4^- ions to its surface. While at alkaline condition, negative charge covers the surface of FAGA due to proton abstraction, thus repelling the CrO_4^{2-} ions and lowering the removal efficiency. On the other hand, the surface of FAGA could be corroded at acidic conditions, which can in turn increase its specific surface area and uncover part of the active sites located in the interior of FAGA. Therefore,

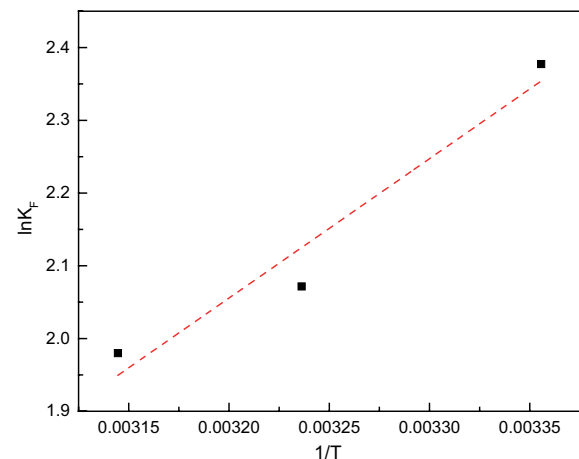


Fig. 6. Adsorption reaction fitting curve of Gibbs equation.

Table 6
Thermodynamic parameters

ΔH° (kJ/mol)	ΔG° (kJ/mol)			ΔS° (J/mol K)	R^2
	298 K	308 K	318 K		
-13.936	-5.832	-5.460	-5.154	-33.905	0.950

the removal efficiency at lower pH condition is more favorable. Yue et al. [8] has found that the maximum adsorption capacity of Cr(VI) using chitosan-coated FA composite as adsorbent was 33.27 mg/g at pH 5.0, and it decreased to 29.73 and 26.86 mg/g at pH of 2.0 and 8.0, respectively. Ballav et al. [52] used polypyrrole-coated halloysite nanotube clay to remove Cr(VI) and found that the removal efficiency was more than 95.0% at pH of 2.0–6.0. All these results from previous works and our results seem to indicate that the removal of Cr(VI) is more favorable at acidic conditions.

3.6. The effect of FAGA dosage

The effect of FAGA dosage on Cr(VI) removal was explored at room temperature (298 K) and a pH value of 5 using various doses (0.1–5.0 g/L). The initial concentration of Cr(VI) was 40 mg/L, and the contact time was 100 min. The experimental results are shown in Fig. 8. The results showed that the removal efficiency increased from around 58.23% to 92.57% as the FAGA dosage increased from 0.1 to 5.0 g/L. This is because at low FAGA dosages, the available active sites are not enough to take all available Cr(VI) in the solution [3]. A sharp increase in removal efficiency is observed as the FAGA dose increases from 0.2 to 2.0 g/L, while insignificant increase is noticed as the FAGA dose increases from 2.0 to 5 g/L.

In contrast, the adsorption capacity decreased as we increased the FAGA dosage, in agreement with previous reports by Zhao et al. [59] and Baral et al. [60] on other similar systems. The larger FAGA dosage increases the available active sites in the adsorption system, but reduces the utilization rate per unit area of FAGA [50].

3.7. The effect of interfering ions

The effect of interfering ions on Cr(VI) adsorption was explored at room temperature (298 K) and a pH value of 5 using FAGA dosages of 2.0 g/L. The initial concentration of Cr(VI) was 40 mg/L (about 0.77 mol/L), and the contact time was 100 min. NaCl and Na₂SO₄ were used to adjust the concentration of Cl⁻ and SO₄²⁻ in the Cr(VI) solution at 0.1, 0.5, 1.0 and 2.0 mol/L. The experimental results are shown in Fig. 9.

It can be seen from Fig. 9 that when the concentration of Cl⁻ is 0.1 mol/L, the removal efficiency decreases by only 0.1%. However, when the concentration of Cl⁻ increases to 2.0 mol/L, the removal efficiency decreases sharply, from 89.41% at 0.5 mol/L to 84.51% at 2.0 mol/L. The effect of SO₄²⁻ on the removal efficiency of Cr(VI) is higher than that of Cl⁻. The removal efficiency decreases by 11.96% when the concentration of SO₄²⁻ is 2.0 mol/L, while this number was only 8.39% for Cl⁻. As reported by Weng et al. [51], higher charged negative ions have a significant influence on the removal efficiency of Cr(VI) because these ions enjoyed higher combining capacity with HCrO₄⁻. This can not only

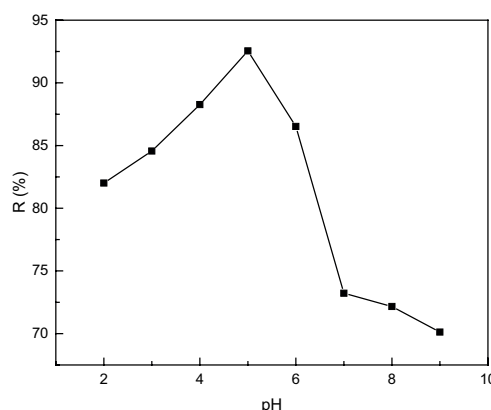


Fig. 7. The influence of pH on the removal efficiency.

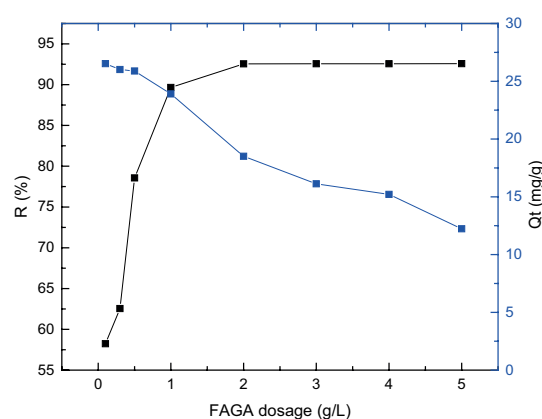


Fig. 8. The influence of FAGA dosage on the removal efficiency and adsorption capacity.

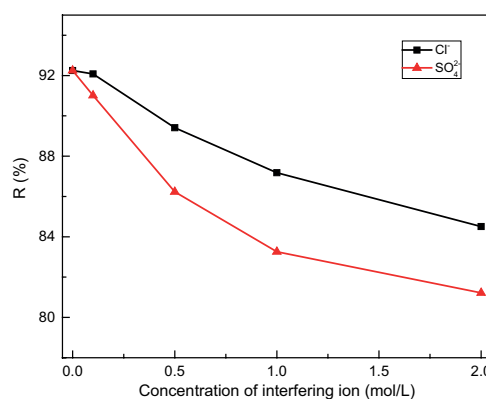


Fig. 9. The influence of interfering ions on the removal efficiency.

Table 7
The energy of adsorption from different forces (kJ/mol)

Van der Waals' force	Hydrogen bond	Dipolar bond	Chemical bond	Coordination exchange	Hydrophobic bond
4–10	2–40	2–29	>60	60	5

lead to competitive adsorption but also compress the double electrode layer between adsorbent and adsorbate and thus influence the normal adsorption process.

Therefore, the interfering ions can disturb the adsorption process, and in our work, in particular, we found that the influence of SO_4^{2-} on the adsorption of Cr(VI) was higher than Cl^- due to the higher negative charge. Therefore, these interfering ions should be removed before putting FAGA into use in order to ensure the best adsorption efficiency.

4. Conclusions

The FAGA has been successfully prepared in the present study. Based on our work, the following conclusions are made:

- From the results of the orthogonal array test, the optimum preparation conditions of FAGA were: $\text{NaOH}/\text{Na}_2\text{SiO}_3$ mass ratio of 2.0, alkali activator/FA mass ratio of 0.5 and a curing temperature of 60°C .
- The kinetic data obtained showed that pseudo-second-order equations controlled the adsorption process. Moreover, according to adsorption isotherm investigations, the Langmuir isotherm model proved to be the best in fitting the adsorption process.
- The negative values of ΔG° suggests that the adsorption of Cr(VI) was a feasible and spontaneous process. On the other hand, ΔG° increased as a function of temperature, coupled with a negative value of ΔS° , indicating that the adsorption process was exothermic. Furthermore, from the value of ΔH° (-13.936 kJ/mol), the adsorption for Cr(VI) onto FAGA was mainly a physical adsorption-based process could be reached.
- The removal efficiency was found to increase as a function of FAGA dosage and reach its maximum at 2.0 g/L, after which the removal efficiency remained stable. The adsorption process was found to be more favorable at acidic conditions with an optimum pH value of 6.
- SO_4^{2-} was found to have a greater influence on the removal efficiency of Cr(VI) than Cl^- . When the concentration of SO_4^{2-} and Cl^- was 2 mol/L, the removal efficiency of Cr(VI) decreased by 11.96% and 8.39% in comparison with the control sample.

Acknowledgment

The authors gratefully acknowledge the financial support from National Sci-Tech Support Plan, 2012BAJ17B01 and 2012BAJ17B02.

References

- [1] Z. Hu, L. Lei, Y. Li, Y. Ni, Chromium adsorption on high-performance activated carbons from aqueous solution, *Sep. Purif. Technol.*, 31 (2003) 13–18.
- [2] Z.C. Di, J. Ding, X.J. Peng, Y.H. Li, Z.K. Luan, J. Liang, Chromium adsorption by aligned carbon nanotubes supported ceria nanoparticles, *Chemosphere*, 62 (2006) 861–865.
- [3] M.S. Al-Harashsheh, K. Al Zboon, L. Al-Makhadmeh, M. Hararah, M. Mahasneh, Fly ash based geopolymer for heavy metal removal: a case study on copper removal, *J. Environ. Chem. Eng.*, 3 (2015) 1669–1677.
- [4] H. Javadian, F. Ghorbani, H.-a. Tayebi, S.H. Asl, Study of the adsorption of Cd (II) from aqueous solution using zeolite-based geopolymer, synthesized from coal fly ash; kinetic, isotherm and thermodynamic studies, *Arab. J. Chem.*, 8 (2015) 837–849.
- [5] M.N. Mužek, S. Svilović, J. Zelić, Fly ash-based geopolymeric adsorbent for copper ion removal from wastewater, *Desal. Wat. Treat.*, 52 (2013) 2519–2526.
- [6] T. Luukkonen, M. Sarkkinen, K. Kemppainen, J. Rämö, U. Lassi, Metakaolin geopolymer characterization and application for ammonium removal from model solutions and landfill leachate, *Appl. Clay Sci.*, 119 (2015) 226–276.
- [7] D. Medpelli, R. Sandoval, L. Sherrill, K. Hristovski, D.-K. Seo, Iron oxide-modified nanoporous geopolymers for arsenic removal from ground water, *Resour.-Effic. Technol.*, 1 (2015) 19–27.
- [8] Y. Wen, Z. Tang, Y. Chen, Y. Gu, Adsorption of Cr(VI) from aqueous solutions using chitosan-coated fly ash composite as adsorbent, *Chem. Eng. J.*, 175 (2011) 110–116.
- [9] V.G. Georgieva, M.P. Tavlieva, S.D. Genieva, L.T. Vlaev, Adsorption kinetics of Cr(VI) ions from aqueous solutions onto black rice husk ash, *J. Mol. Liq.*, 208 (2015) 219–226.
- [10] M. Ji, X. Su, Y. Zhao, W. Qi, Y. Wang, G. Chen, Z. Zhang, Effective adsorption of Cr(VI) on mesoporous Fe-functionalized Akadama clay: optimization, selectivity, and mechanism, *Appl. Surf. Sci.*, 344 (2015) 128–136.
- [11] Y. Zhao, W. Qi, G. Chen, M. Ji, Z. Zhang, Behavior of Cr(VI) removal from wastewater by adsorption onto HCl activated Akadama clay, *J. Taiwan Inst. Chem. Eng.*, 50 (2015) 190–197.
- [12] Z. Zhang, J.L. Provis, J. Zou, A. Reid, H. Wang, Toward an indexing approach to evaluate fly ashes for geopolymer manufacture, *Cem. Concr. Res.*, 85 (2016) 163–173.
- [13] J. Xie, O. Kayali, Effect of superplasticiser on workability enhancement of Class F and Class C fly ash-based geopolymers, *Constr. Build. Mater.*, 122 (2016) 36–42.
- [14] B. Singh, M.R. Rahman, R. Paswan, S.K. Bhattacharyya, Effect of activator concentration on the strength, ITZ and drying shrinkage of fly ash/slag geopolymer concrete, *Constr. Build. Mater.*, 118 (2016) 171–179.
- [15] M. Babae, A. Castel, Chloride-induced corrosion of reinforcement in low-calcium fly ash-based geopolymer concrete, *Cem. Concr. Res.*, 88 (2016) 96–107.
- [16] A.A. Aliabdo, A.E.M. Abd Elmoaty, H.A. Salem, Effect of water addition, plasticizer and alkaline solution constitution on fly ash based geopolymer concrete performance, *Constr. Build. Mater.*, 121 (2016) 694–703.
- [17] T. Aldahri, J. Behin, H. Kazemian, S. Rohani, Synthesis of zeolite Na-P from coal fly ash by thermo-sonochemical treatment, *Fuel*, 182 (2016) 494–501.
- [18] Q. Zhou, C. Yan, W. Luo, Polypyrrole coated secondary fly ash-iron composites: novel floatable magnetic adsorbents for the removal of chromium (VI) from wastewater, *Mater. Des.*, 92 (2016) 701–709.
- [19] M. Ahmaruzzaman, A review on the utilization of fly ash, *Prog. Energy Combust. Sci.*, 36 (2010) 327–363.
- [20] C.F. Wang, L.J. Wang, X.Y. Sun, Adsorption of dye from wastewater by zeolites synthesized from fly ash: kinetic and equilibrium studies, *Chin. J. Chem. Eng.*, 17 (2009) 513–521.
- [21] C.F. Wang, J.S. Li, X. Sun, L.J. Wang, Evaluation of zeolites synthesized from fly ash as potential adsorbents for wastewater containing heavy metals, *J. Environ. Sci.*, 21 (2009) 127–136.
- [22] R. Kikuchi, Application of coal ash to environmental improvement: transformation into zeolite, potassium fertilizer, and FGD absorbent, *Resour. Conserv. Recycl.*, 27 (1999) 333–346.
- [23] H. Cheng, K.L. Lin, R. Cui, C.L. Wang, T.W. Cheng, Y.M. Chang, Effect of solid-to-liquid ratios on the properties of waste catalyst–metakaolin based geopolymers, *Constr. Build. Mater.*, 88 (2015) 74–83.
- [24] H. Cheng, K.L. Lin, R. Cui, C.L. Wang, Y.M. Chang, T.W. Cheng, The effects of $\text{SiO}_2/\text{Na}_2\text{O}$ molar ratio on the characteristics of alkali-activated waste catalyst–metakaolin based geopolymers, *Constr. Build. Mater.*, 95 (2015) 710–720.
- [25] C. Bobirić, J.H. Shim, J.H. Pyeon, J.Y. Park, Influence of waste glass on the microstructure and strength of inorganic polymers, *Ceram. Int.*, 41 (2015) 13638–13649.

- [26] G. Görhan, G. Kürklü, The influence of the NaOH solution on the properties of the fly ash-based geopolymer mortar cured at different temperatures, *Composites Part B*, 58 (2014) 371–377.
- [27] C. Yang, C. Cui, J. Qin, Recycling of low-silicon iron tailings in the production of lightweight aggregates, *Ceram. Int.*, 41 (2015) 1213–1221.
- [28] D.C. Fan, W. Ni, A.Y. Yan, J.Y. Wang, W.Y. Cui, Orthogonal experiments on direct reduction of carbon-bearing pellets of Bayer red mud, *J. Iron Steel Res. Int.*, 22 (2015) 686–693.
- [29] F.L. da Silva, F.G.S. Araújo, M.P. Teixeira, R.C. Gomes, F.L. von Krüger, Study of the recovery and recycling of tailings from the concentration of iron ore for the production of ceramic, *Ceram. Int.*, 40 (2014) 16085–16089.
- [30] P. Chindaprasirt, U. Rattanasak, S. Taebuanhuad, Role of microwave radiation in curing the fly ash geopolymer, *Adv. Powder Technol.*, 24 (2013) 703–707.
- [31] S. Aydın, B. Baradan, Mechanical and microstructural properties of heat cured alkali-activated slag mortars, *Mater. Des.*, 35 (2012) 374–383.
- [32] D. Xu, Adsorption of Pb(II) from aqueous solution to MX-80 bentonite: effect of pH, ionic strength, foreign ions and temperature, *Appl. Surf. Sci.*, 41 (2008) 37–46.
- [33] K. Al-Zboon, M.S. Al-Harabsheh, F.B. Hani, Fly ash-based geopolymer for Pb removal from aqueous solution, *J. Hazard. Mater.*, 188 (2011) 414–421.
- [34] Y.S. Zhang, W. Sun, Z.J. Li, Composition design and microstructural characterization of calcined kaolin-based geopolymer cement, *Appl. Surf. Sci.*, 47 (2010) 271–275.
- [35] A.M.M.A. Bakria, H. Kamarudin, M. BinHussain, I.K. Nizar, Y. Zarina, A.R. Rafiza, The effect of curing temperature on physical and chemical properties of geopolymers, *Phys. Procedia*, 22 (2011) 286–291.
- [36] F.G.M. Aredes, T.M.B. Campos, J.P.B. Machado, K.K. Sakane, G.P. Thim, D.D. Brunelli, Effect of cure temperature on the formation of metakaolinite-based geopolymer, *Ceram. Int.*, 41 (2015) 7302–7311.
- [37] X. Ma, Z. Zhang, A. Wang, The transition of fly ash-based geopolymer gels into ordered structures and the effect on the compressive strength, *Constr. Build. Mater.*, 104 (2016) 25–33.
- [38] M. Chi, Y. Liu, R. Huang, Mechanical and microstructural characterization of alkali-activated materials based on fly ash and slag, *Int. J. Eng. Technol.*, 7 (2015) 59–64.
- [39] N. Böke, G.D. Birch, S.M. Nyale, L.F. Petrik, New synthesis method for the production of coal fly ash-based foamed geopolymers, *Constr. Build. Mater.*, 75 (2015) 189–199.
- [40] Z. Zhang, J.L. Provis, A. Reid, H. Wang, Fly ash-based geopolymers: the relationship between composition, pore structure and efflorescence, *Cem. Concr. Res.*, 64 (2014) 30–41.
- [41] D. Panias, I.P. Giannopoulou, T. Perraki, Effect of synthesis parameters on the mechanical properties of fly ash-based geopolymers, *Colloids Surf., A*, 301 (2007) 246–254.
- [42] K.K. Al-Zboon, B.M. Al-smadi, S. Al-Khawaldh, Natural volcanic tuff-based geopolymer for Zn removal: adsorption isotherm, kinetic, and thermodynamic study, *Water Air Soil Pollut.*, 227 (2016) 1–22.
- [43] S. Kumar, R. Kumar, Mechanical activation of fly ash: effect on reaction, structure and properties of resulting geopolymer, *Ceram. Int.*, 37 (2011) 533–541.
- [44] M.M. Al Bakri Abdullah, K. Hussin, M. Bnhussain, K.N. Ismail, Z. Yahya, R.A. Razak, Fly ash-based geopolymer lightweight concrete using foaming agent, *Int. J. Mol. Sci.*, 13 (2012) 7186–7198.
- [45] Y. Yao, H. Sun, A novel silica alumina-based backfill material composed of coal refuse and fly ash, *J. Hazard. Mater.*, 213–214 (2012) 71–82.
- [46] M. Kumari, C.U. Pittman Jr., D. Mohan, Heavy metals [chromium (VI) and lead (II)] removal from water using mesoporous magnetite (Fe₃O₄) nanospheres, *J. Colloid Interface Sci.*, 442 (2015) 120–132.
- [47] Z. Liu, Cr⁶⁺ adsorption mechanism on ultrafine coal fly ashes and its kinetics, *J. Chin. Univ. Mining Tech.*, 37 (2008) 478–482.
- [48] Y.Y. Ge, X.M. Cui, Y. Kong, Z.L. Li, Y. He, Q.Q. Zhou, Porous geopolymeric spheres for removal of Cu (II) from aqueous solution: synthesis and evaluation, *J. Hazard Mater.*, 283 (2015) 244–251.
- [49] C. Wang, L. Boithias, Z. Ning, Y. Han, S. Sauvage, J.-M. Sánchez-Pérez, K. Kuramochi, R. Hatano, Comparison of Langmuir and Freundlich adsorption equations within the SWAT-K model for assessing potassium environmental losses at basin scale, *Agric. Water Manage.*, 180 (2016) 205–211.
- [50] R. Xin, Preparation of Adsorbents from Water Treatment Plant Wastewater Sludge and the Removal Efficiency for Hexavalent Chromium, Harbin Institute of Technology, Harbin, 2014, p. 117.
- [51] C.H. Weng, Y.C. Sharma, S.H. Chu, Adsorption of Cr(VI) from aqueous solutions by spent activated clay, *J. Hazard. Mater.*, 155 (2008) 65–75.
- [52] N. Ballav, H.J. Choi, S.B. Mishra, A. Maity, Polypyrrole-coated halloysite nanotube clay nanocomposite: synthesis, characterization and Cr(VI) adsorption behaviour, *Appl. Clay Sci.*, 102 (2014) 60–70.
- [53] M.H. Dehghani, D. Sanaei, I. Ali, A. Bhatnagar, Removal of chromium(VI) from aqueous solution using treated waste newspaper as a low-cost adsorbent: kinetic modeling and isotherm studies, *J. Mol. Liq.*, 215 (2016) 671–679.
- [54] X. Wang, C. Wu, L. Tian, G. Li, X. Zhang, F. Lei, J. Qu, P. Liu, Cationic polymer chain tethered on the pore-wall of 3-D ordered macroporous resin for the removal of hexavalent chromium from aqueous solution, *React. Funct. Polym.*, 95 (2015) 55–61.
- [55] R. Donat, A. Akdogan, E. Erdem, H. Cetisli, Thermodynamics of Pb²⁺ and Ni²⁺ adsorption onto natural bentonite from aqueous solutions, *J. Colloid Interface Sci.*, 286 (2005) 43–52.
- [56] M. Khitous, Z. Salem, D. Halliche, Effect of interlayer anions on chromium removal using Mg-Al layered double hydroxides: kinetic, equilibrium and thermodynamic studies, *Chin. J. Chem. Eng.*, 24 (2016) 433–445.
- [57] F.V. Hackbarth, D. Maass, A.A.U. de Souza, V.J.P. Vilar, S.M.A.G.U. de Souza, Removal of hexavalent chromium from electroplating wastewaters using marine macroalga *Pelvetia canaliculata* as natural electron donor, *Chem. Eng. J.*, 290 (2016) 477–489.
- [58] J. Augustynowicz, J. Kyzioł-Komosińska, W. Lasek, Removal of chromium species from waters by Callitriche, *New Biotechnol.*, 33 (2016) S31.
- [59] N. Zhao, N. Wei, J. Li, Z. Qiao, J. Cui, F. He, Surface properties of chemically modified activated carbons for adsorption rate of Cr (VI), *Chem. Eng. J.*, 115 (2005) 133–138.
- [60] S.S. Baral, S.N. Das, P. Rath, G.R. Chaudhury, Chromium(VI) removal by calcined bauxite, *Biochem. Eng. J.*, 34 (2007) 69–75.